sciendo

CIVIL AND ENVIRONMENTAL ENGINEERING REPORTS

E-ISSN 2450-8594

CEER 2019; 29 (4): 218-235
DOI: 10.2478/ceer-2019-0056

Original Research Article

THERMODYNAMIC ASSESSMENT ON THE INTEGRATION OF THERMO-ELECTRIC MODULES IN A WOOD FIREPLACE

Andrea BALDINI[2], Luca CEROFOLINI[2], Daniele FIASCHI[1], Giampaolo MANFRIDA[1], Lorenzo TALLURI[1]

[1]University of Florence, Firenze, Italy

[2]OffgridBox®, Somerville, USA

Abstract

The growing demand for electricity produced from renewable sources and the development of new technologies for the combustion of biomass, arose a growing interest on the possible coupling of thermoelectric modules with stove-fireplaces.

The current thermoelectric generators have a solid structure, do not produce noise, do not require maintenance and can be used for the recovery of waste heat or excess, at the same time they hold a very low conversion efficiency and they need an adequate cooling system. Nevertheless, they still hold a cost, which is still too high to make them attractive. Nonetheless, if the modules are applied to a heat source which otherwise would be wasted, the attractiveness of the solution certainly rises.

In this study, a thermodynamic analysis of a stove-fireplace is presented, considering both combustion process and the flame – walls heat transfer of the. A design solution for a concentrator device to funnel the wasted heat from the fireplace to the thermo-electric modules is also presented.

Keywords: thermo-electric modules, stove-fireplace, thermodynamic assessment

[1] Corresponding author: University of Florence, Department of Industrial Engineering, Firenze, Italy, e-mail: giampaolo.manfrida@unifi.it, tel. 0552758676

1. INTRODUCTION

Recent years have seen the increasing diffusion of smart distributed energy systems [1, 2]. In countries where radiation conditions are attractive, Solar Photovoltaic has become a major contributor, with over 100 GW installed in Europe and aiming at 1000 GW worldwide level for 2022 [3]. Countries like Italy had a very strong growth until 2013 because of favourable incentives, reaching a significant contribution of Solar PV to the overall Italian electricity balance (24,000 GWh in 2017 – about 7.5% of the national electricity consumption). It is well known that the increasing market share of renewable is putting severe challenges to the national and European grids: in this light, solar energy (compared to wind or wave energy) has on its side the daily cycle and a good predictability, however the result is that in countries like Italy the highest cost of electricity is registered since 2012 in the evening. Referring to Italy, 90% of the PV plants have a nominal capacity below 20 kW and their contribution to the overall PV production is about 4.8 GWh (20% share) [4]. Most of these PV plants are private-owned, serving households, farms or small industrial activities.

An increasing share of people who have installed PV plants is attracted by the possibility of gaining autonomy from the grid. This happens because the incentives have decreased, so that at present grid parity (yearly consumption = production) is in practice required; even in these conditions, the cost of on-site exchange and load mismatch compensation is relevant. Moreover, a number of applications exist (isolated households or tourist resorts, small villages, agritourisms, etc.) who are committed to go off-grid, or build local isolated micro grids with capability of load compensation. This is indeed the mission of OffGridBox® [5], an international start up born in 2017 after pilot experimentation in Italy and in several emergency or international cooperation projects since 2010. The main product of OffGridBox® is a container equipped with a small PV field; the container can be supplied with different equipment for helping the needs of the local users: usually a water purification (or desalination) system, but also the complete and ready-to-use electric control system, including batteries or other types of energy storage (electricity and thermal). The users of OffGridBox® have the problem of guaranteeing continuity of electricity after sunset: this is usually provided by batteries. In applications of EU climate, the same users often have installed (or plant to install) a biomass household heating system with integrated storage. The solution is generally a fireplace with integrated sanitary water reservoir, which is connected to the household heating and sanitary water system.

The idea of adding the capability of thermo-electric (TE) power generation to the fireplace is very attractive and challenging. The conditions appear to be

favourable: the size of the combustion chamber is larger than in pellet or wood chip stoves, and a relevant part of the fireplace is working on radiation principles which allow to reach the high energy flux need by TE modules. On the cold side, heat removal from the modules can profit of the good heat transfer coefficient using water as heat transfer medium. It was thus decided to run a sizing exercise through the development of a model, using the standing cooperation with University of Florence, Italy.

2. THERMO-ELECTRIC POWER GENERATION

Thermo electric modules allows the conversion of wasted heat to electricity in a very environmental friendly way. Indeed, the TE cells are in a solid state, avoiding therefore any gas emissions [6]. Furthermore, they also have the very valuable benefits of being scalable, of not requiring any maintenance, and of not having any moving particles or chemical reactions for producing electricity. Therefore, the possibility of using such systems to build small power units for distributed power generation has attracted the attention of several researchers. In order to demonstrate the technical feasibility, models have been realized (mainly for the electrical section) and prototypes built. Champier et al. [7] proposed the use of TE modules in a small cooking oven, demonstrating the possibility of producing 8 W using 4 TE modules in series. The modules where air-cooled on the cold side, using a large finned heat dissipater. Subsequent work by the same research group [8] positioned the TE generator below the hot water storage unit in order to increase the convective heat flux to the TE module; a comprehensive model of heat transmission across the module was introduced, including equations describing the electrical characteristic of the TE module. Good agreement between model and experiments was found, with a power output limited to 10W.
Zheng et al. [9] investigated direct thermo-electric power generation from heat developing a model and performing some lab-scale tests on a small bench (electric oven). The effect of a possible widespread application of TE technology to domestic boilers in UK is evaluated, evaluating a payback period of about 5,6 yrs.
More extensive small-scale tests are reported in [10], achieving an overall conversion efficiency of about 4% with a temperature difference close to 150°C between the hot source and the cold sink.
Barma et al. [11] evaluated the possibility of thermo-electric power generation recovering heat from the flue gases of a large (14MW) biomass-fired oil heating unit; the TE modules are cooled by air through the use of a finned back dissipator. A mathematical model of the electric section is developed, with appropriate hypotheses for the heat transfer. The system is proposed to operate with a hot source temperature of 573K, with a considerable number of TE modules (>2400),

achieving a calculated maximum output of 4 W/module. Different materials for the TE modules are considered.

Montecucco et al. [12, 13] developed a Matlab model for thermoelectric power generation, including heat transfer and electrical effects; the model includes geometric optimization of the internal layout of the module in order to improve the performance.

Bianchini et al. [14] developed a test bench for experimental qualification of TE modules, to be applied with convective heat transfer on the hot side and applying water cooling for heat removal. The test results reach a temperature difference of 250°C and demonstrate a power output of nearly 30W for one single module (75*75 mm) with a characteristic curve showing an evident power improvement trend with increasing operating temperature difference.

Nuwayhid et al. [15] have presented a power generating system with a TEG fitted to the side of a domestic woodstove and cooled by natural convection (using a heat sink). The maximum matched load power in a steady state, achieved using a single module, was 4.2W. Nuwayhid et al. [16] also considered the possibility of continuous generation of 10–100W of electric power using the heat from 20 to 50 kW wood stoves. In the first prototype, the maximum achieved power per module was at the level of 1W (using low-cost Peltier modules). This was caused by the low temperature difference (limited by the maximum operation temperature of the modules) and by the geometry that was not optimized for power generation. Lertsatitthanakorn investigated a similar prototype based on a biomass cooking stove, achieving a power output of 2.4 W; the economic analysis indicated that its payback time could be very short [17]. As opposed to air cooling systems, Rinalde et al. [18] studied a forced water cooling system. In his study, an electric heater was used as a heat source and the maximum power obtained was at the level of 10 W. Faraji et al. [19] recommended a TE system configuration with the heat removed through water, resulting in a much more compact solution than that with air cooling. The enhancement of the heat exchanged and also of the efficiency of the TE modules by utilizing water instead of air was also assessed by Du et al. [20], where in their work an experimental campaign was conducted in order to demonstrate that a water cooling solution is more advantageous than an air cooled one. Other experimental campaigns were performed by Liu et al. [21], where several materials and boundary conditions were assessed, obtaining a maximum 500 W power output for a 96 TE module configuration. Sornek et al. [22], developed a feasibility study on the potential utilization of TE power generator applied to stove-fireplaces with heat accumulation systems. In their study the maximum experimental power obtained was of 6 W, achieved in a representative designed test rig. Ding et al. [23] developed an experimental campaign on the application of TE modules to a domestic natural gas water heater in order to

recover part of the wasted heat. The maximum achieved power was of 42.4 W for a 60 module configuration. Obernberger et al. [24] realized a small scale CHP technology integrating the TE modules inside a wood pellet stove of 10.5 kW thermal capacity. The objective of their study was to demonstrate the feasibility of utilizing such systems in an off-grid scenario.
On the whole, it appears that efforts of researchers were directed to demonstrating the practical operation of a TE system integrated (in most cases) with a stove, adapting existing TE modules to an existing stove with minor adjustments. This lead to very low power levels, mainly because of limits determined by the air cooling of the back side of the modules, or of limited temperature difference and heat flux. In the following, we will show how to take advantage of the high heat flux possible through radiation, in the context of a closed fireplace layout which appears favourable in terms of available internal surface.

3. LAYOUT OF THE FIREPLACE UNIT – TE DESIGN ADAPTATION

A fireplace for comfort heat and production for sanitary water for a household has a typical power rating of 20 kWt; the overall size of the commercial unit here considered, which incorporates a large heat capacity of about 0.4 m^3 placed above the combustion chamber, is about 1.0W*0.70D*1.60H [m]. The atmospheric-pressure water storage is heated by a multi-pass firetube arrangement; typical temperatures in the range of 60-80°C are reached and direct pipe connections to the comfort heating and sanitary water system are provided. A schematic of the current arrangement of the fireplace with integrated water storage is shown in Figure 1. From the constraints imposed by the existing layout, and considering the problems encountered by the cited researchers, who all tried to design a system based on convective heat transfer on the hot side, it was decided to drive the re-design of the fireplace in order to achieve high-flux radiative heat transfer to the TE section.
The combustion chamber has a size of 0.78W*0.50D*0.43H [m], and is separated from the room by a front quartz glass window. The side faces (1, 2, 3; having the TE modules on the back side) are considered manufactured from cast iron or CORTEN, having $\varepsilon = 0.9$; the upper and lower sides (4, 5) are built with a silica-based refractory liner having low emissivity ($\varepsilon = 0.4$). About 25% of the upper wall is occupied by the exhaust gas port, which leads to the multi-pass fire-tube heat exchanger for water heating.

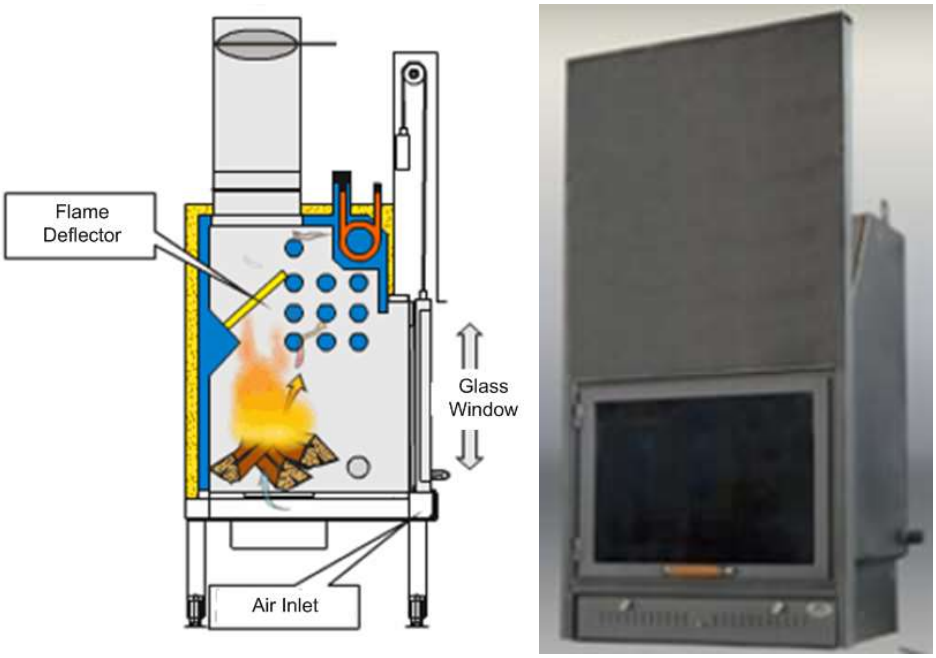

Fig. 1. Schematic (a) and photo (b) of household fireplace with integrated hot water storage

4. MODEL OF THE THERMO-ELECTRIC FIREPLACE

The model of the thermo-Electric fireplace is composed of several logical coupled sections:

1. model of the combustion chamber
2. combustion chamber radiation model
3. glass window selectivity
4. heat transfer to thermo-electric modules
5. heat flux concentrator

4.1. Model of the combustion chamber

The approach to the energy balance of the combustion chamber relies on consolidated practice of industrial furnace modelling though Mullikin's approach [25], with separation of radiation modeling from the flame to the walls or glass window.

The overall heat radiated from the flame (0) to the 6 CC walls is:

$$Q_{irr} = \sum_1^6 Q_{irr,\ 0,\ i} \qquad i=1\ldots6 \qquad (4.1)$$

The flame temperature T_g was assumed constant across the combustion chamber and equal to the flame temperature T_f (one-zone model).
The heat entering the system is determined by the wood consumption rate of the fireplace, which was estimated at 5 kg/h (corresponding to a nominal power of about 27 kW and a calorific value of 16,750 kJ/kg); it was assumed that under correct air flow control $\alpha = 7 \frac{kg_{air}}{kg_W}$.

$$Q_{in} = \dot{m}_w\left(H_i + \alpha c_{p;a} T_a\right) \tag{4.2}$$

The sensible heat flow exiting the combustion chamber with the hot combustion gases is given by:

$$Q_u = \dot{m}_w(1 + \alpha) c_{p;g} T_g \tag{4.3}$$

The combustion chamber balance can be written as:

$$Q_{in} - Q_{irr} - Q_u = 0 \tag{4.4}$$

Eq. 4 results to be a 4th-order equation in terms of T_g, which can be solved by a simple numerical procedure (minimization of residual). Figure 2 displays the notation of the walls of the schematized fireplace.

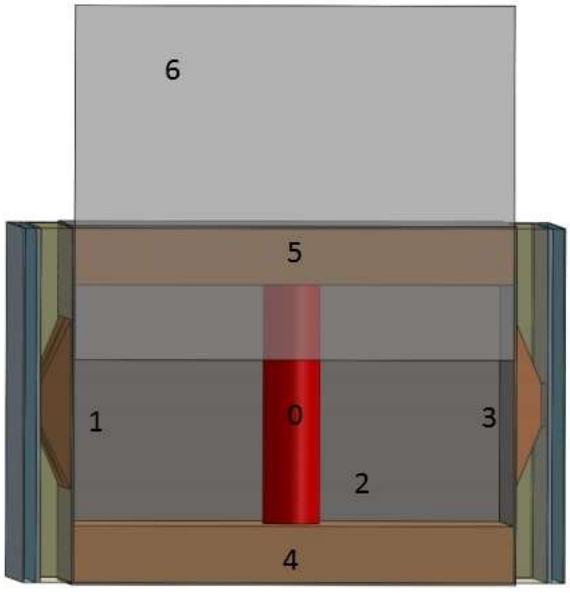

Fig. 2. Schematic fireplace with walls notation

4.2. Combustion chamber radiation modelling

The flame is conceptually replaced by a cylindrical radiating body (0) (D_f = 0.1 m) with emissivity ε_f = 0.85 (corresponding to a typical wood fire). Each radiation heat rate is evaluated separately, considering both radiation from flame to the walls, and radiation among walls at different temperatures considering the geometrical view factors.

$$Q_{irr,i,j} = \sigma S_i \, VF_{j,i}(\varepsilon_i T_i^4 - \varepsilon_i T_j^4) \qquad i, j = 1 \ldots 6 \qquad (4.5)$$

$$Q_{irr,0} = \sum_{j=1}^{6} Q_{irr,0,j} \qquad j = 1 \ldots 6 \qquad (4.6)$$

The view factors were calculated first for the empty combustion chamber and then for the complete radiation setup including the cylindrical grey body equivalent to the flame. The view factors are first evaluated for the combustion chamber only (no flame), resulting in a symmetric matrix. After that the view factor of the flame (assumed as an equivalent cylinder) with respect to the walls is evaluated. This last matrix is subtracted from the previous one exploiting the additive properties of radiation; the final matrix is non-symmetric in strict terms, due to the difference in area between the flame and the walls, but maintains some fundamental symmetric behaviour (left/right = 1/3 and up/down = 4/5). The resulting view factor matrix is reported in Table 1. Eq. 6 (defining the heat radiated by the flame) provides the necessary input for the energy balance (Eqs. 1 and 4), and together with them it allows to calculate the flame temperature T_f.

Table 1. Calculated view factors VF*i,j* for the given geometry

i \ *j*	*0*	*1*	*2*	*3*	*4*	*5*	*6*
0	*0*	*0.1213*	*0.1575*	*0.1213*	*0.2212*	*0.2212*	*0.1575*
1	*0.07636*	*0*	*0.21*	*0.01515*	*0.2442*	*0.2442*	*0.21*
2	*0.06369*	*0.1349*	*0*	*0.1349*	*0.2501*	*0.2501*	*0.1663*
3	*0.07636*	*0.01515*	*0.21*	*0*	*0.2442*	*0.2442*	*0.21*
4	*0.07635*	*0.1339*	*0.2135*	*0.1339*	*0*	*0.2288*	*0.2135*
5	*0.07635*	*0.1339*	*0.2135*	*0.1339*	*0.2288*	*0*	*0.2135*
6	*0.06369*	*0.1349*	*0.1663*	*0.1349*	*0.2501*	*0.2501*	*0*

The radiation model must be completed with the glass window, which presents a selectivity (ε and τ are a function of T_f) which requires an iterative solution.

4.3. Glass Window selectivity

The radiation intensity is a function of wavelength and of the flame temperature, considering Planck's law for a grey body (flame):

$$E_\lambda(T_f) = \varepsilon_f \frac{C_1}{\lambda^5\left[e^{\frac{C_2}{\lambda T_f}} - 1\right]} \tag{4.7}$$

With C_1 = 3.742 [W*μm4/m2], C_2 = 1.439 x 104 [μm *K].

The emissivity and transmissivity of the glass window have to be determined iteratively as a function of the flame temperature; in fact, as T_f is raised, radiation is displaced to the UV wavelength region and the glass is behaving more and more as a non-transmissive surface; on the other hand, for low T_g the radiation is mainly IR and the glass behaves as a transparent medium. In all cases,

$$\rho + \tau + \alpha = 1 \tag{4.8}$$

Here it was assumed that the glass reflectivity is low (due to soot deposited which prevents the glass from working like a mirror); moreover, Kirchhoff's law allows to approximate under equilibrium conditions:

$$\varepsilon(T_f, \lambda) = \alpha(T_f, \lambda) \tag{4.9}$$

So that combining (6) and (7):

$$\varepsilon(T_f, \lambda) = 1 - \tau(T_f, \lambda) \tag{4.10}$$

Table 2 collects data for quartz glass selectivity taken from a manufacturer [26], which are confirmed by literature data [27].

Table 2. Transmissivity data of quartz silica glass as a function of wavelength [26]

λ, μm	*τ, %*
0.25	0
0.26	0
0.27	2
0.28	3
0.29	15
0.3	35
0.31	65

The overall transmissivity and emissivity of the glass window are finally evaluated as:

$$\tau_{gw} = \frac{\int_0^\lambda \boldsymbol{\tau}(T_f,\lambda)\, E_\lambda(T_f) d\lambda}{\int_0^\lambda E_\lambda(T_f) d\lambda} \tag{4.11}$$

$$\varepsilon_{gw} = 1 - \tau_{gw} \tag{4.12}$$

4.4. Heat transfer to thermoelectric modules

The radiation model allows to calculate the (equivalent average) temperature of each wall, and consequently the heat rate radiated from the flame to the wall; in order to do that, the boundary conditions must be specified in terms of heat flux investing the walls where the TE modules are installed. These represent specified heat flux conditions (walls 1, 2 and 3); on boundaries 4, 5 and 6 (glass) equivalent boundary conditions must be specified (conduction/convection heat loss through the wall or glass). The conduction heat losses (walls 4 and 5) are marginal because these walls are refractory-lined (k_{ref} = 0.25 W/(mK)); the glass window is treated as a thin isothermal layer, with heat flux conditions set by the external radiation and natural convection (hot vertical plate) heat losses:

$$Q_{irr,0,6} = Q_{gw,a} = \frac{\sigma S_{gw} (T_{gw}{}^4 - T_j{}^4)}{1 + {(1-\varepsilon_{gw})}/{\varepsilon_{gw}}} + h_{VP} S_{gw} \left(T_{gw} - T_a\right) \quad (4.13)$$

On the walls hosting on the back side the TE modules, a high-conductivity cast iron layer (k_{pi} =55 W/(mK); s_{pi} = 0.01 m) is adopted in order to promote heat transfer to the TE modules. These last were selected based on market availability: the TE modules are Hi-Z 20 W units [14, 28] (75*75*5 mm), which can be operated with hot/cold side temperatures $T_{TE,H}$ = 525K and $T_{TE,C}$ =323 K; the cell conductivity is 2.4 W/(m°C), determining a heat flow rate $Q_{in,TE}$ = 527W for each cell. On the whole, as the TE modules can be installed on walls 1,2 and 3, the heat rate balance can be set in the following terms:

$$Q_{irr,0,1} + Q_{irr,0,2} + Q_{irr,0,3} = (n_1 + n_2 + n_3)\, Q_{in,TE}) \quad (4.14)$$

Which determines the solution shown in Table 3. The results appear physically sound: the average (single-zone) flame temperature is Tf = 1100 K; the nearly-adiabatic (refractory-lined, low emissivity) walls 4 and 5 reach a high surface temperature (nearly 800K), while the cooled walls (1, 2 and 3) are maintained to a level of about 550K which is suitable for use on the TE module hot side. The glass window (6) finds its calculated equilibrium temperature at about 564K because of transmissivity (mainly infrared) and external radiation and natural convective cooling.

According to the data sheet, each TE module provides a power according to the thermoelectric characteristic of the module:

$$P = 0{,}0005\,(T_{TE,H} - T_{TE,C})2 = 20\,W \quad (4.15)$$

That, is, with an efficiency of about 3.8% and an overall expected power output from the fireplace of about 140W. The market cost of the 7 modules is about 280$ (that is, about 2,000 €/kW, comparable to that of other renewable such as photovoltaics or medium/small wind turbines).

Table 3. Wall temperatures, Heat rates and number of TE modules

Surface	*T, K*	*Q_{irr}, W*	*A, m^2*	*n_i*
0	*1100*	*0*	*0.134*	-
1	*553.5*	*1066*	*0.213*	*2*
2	*550.6*	*1386*	*0.331*	*2*
3	*553.5*	*1066*	*0.213*	*2-3*
4	*796.1*	*1816*	*0.388*	-
5	*796.1*	*1816*	*0.388*	-
6	*564.6*	*1424*	*0.331*	-

4.5. Conductive heat transfer to the TE module - Heat flux concentrator

The radiation model allows to calculate the average temperature of each wall, and consequently the heat rate radiated from the flame to the wall. The solution also determines the heat flux to be realized on the TE module, which exceeds 90 kW/m^2. This very high heat flux must be produced on the hot and cold sides of the TE module, which requires thus a careful design in terms of conductive (combustion chamber wall to TE module hot side) and convective (TE module cold side to water) heat transfer.

On the TE hot side, an intensification of the radiative heat flux of about 18 times is required. To this end, a special high-conductivity copper heat flux concentrator (HFC) was designed, as shown in Figure 3. The HFC is packaged inside an insulated box, hosting inside also the TE module and the water cooler; the void between the HFC and the box is filled with fine refractory sand, so that heat is preferably transmitted through the high-conductivity copper thermal bridge. Figure 4 displays how the box would be assembled, confirming the feasibility and easiness of the solution, which guarantees a low cost application.

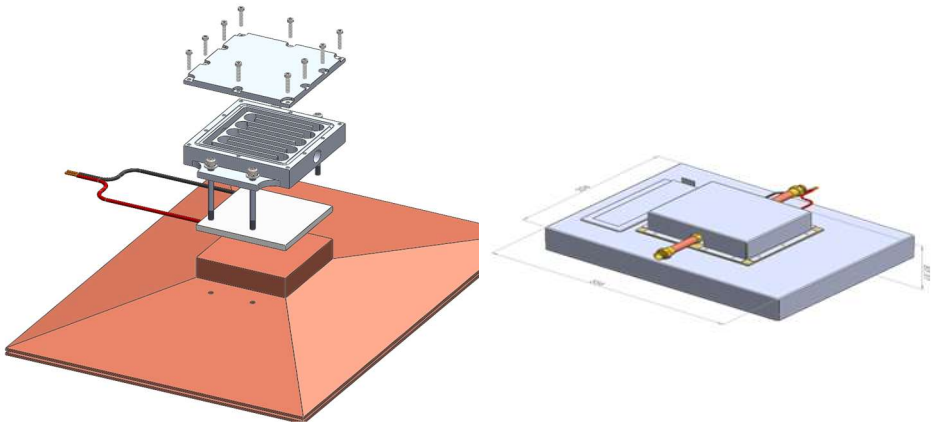

Fig. 3. Heat flux concentrator (HFC), TE module and water cooler assembly

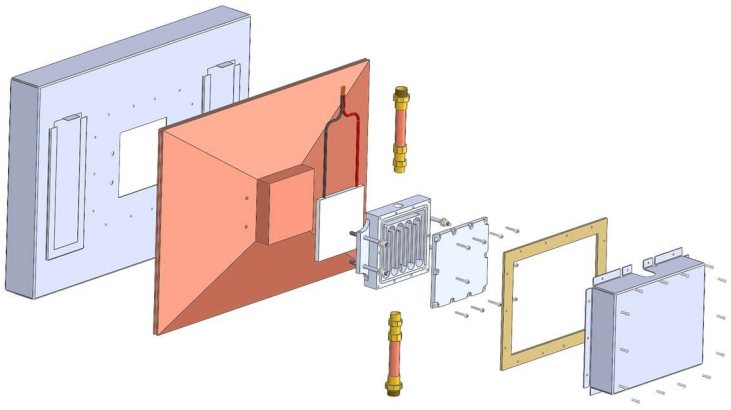

Fig. 4. HFC - TE - HE assembling

On the whole, the TE heat transfer balance is described by the following equations:

$$Q_{in,TE} = \frac{(T_H - T_{CH})}{R_{ov}} \tag{4.16}$$

$$R_{ov} = R_{ci} + R_{Cu} + R_c \tag{4.17}$$

The thermal resistances of the cast iron (ci) and copper (Cu) layers are small, and the contact resistance with the high-temperature wall is managed through a suitable spring loading and possible interposition of a thin soft metal layer. This allows to reach a low value of $R_{ov} \cong 0.12 - 0.19$ K/W.
An important issue is the efficiency of the HFC, defined as

$$\eta_{HFC} = \frac{Q_{HFC,out}}{Q_{HFC,in}} \tag{4.18}$$

Which depends on the longitudinal heat loss through the refractory silica sand layer. In order to determine η_{HFC}, several calculation were performed on conductive heat transfer using ANSYS. Particularly, several geometries of the HFC were examined, as displayed in figure 5. Different geometries gave different temperature profiles on the face of the cell: the objective of the analysis was to assess which was the one that allowed the most homogeneous temperature profile on the surface of the cell. As can be depicted from figure 6 and 7, the configuration which guaranteed an almost uniform distribution on the surface of the HFC in contact with the TE module was conf. 3, with a maximum temperature variation within 0.5°C. The heat flow profiles were then calculated on the centreline of the HFCs and the inlet and outlet thermal powers were calculated; the profiles were variable according to the geometry: where the section decreased, an increase in

the flow was found, as one would expect. Finally, the geometry with the square extension (Conf. 3) was selected due to the characteristic of holding the most uniform temperature profile and has an efficiency slightly lower than the maximum obtained (Conf. 1) so it was considered as an excellent compromise. A further upgrade was the replacing of the silica sand with expanded vermiculite insulator. This resulted in an improvement of the HFC efficiency from 73% to 89%.

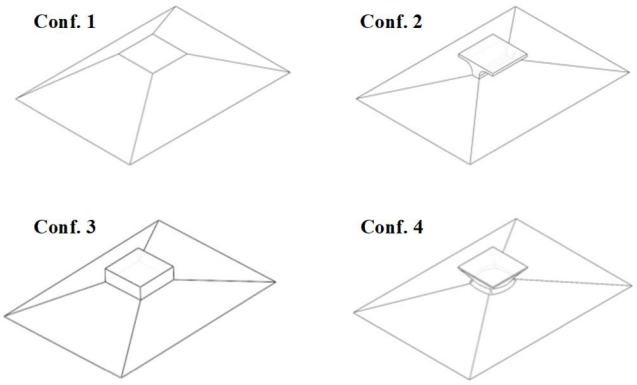

Fig. 5. HFC assessed geoemetries

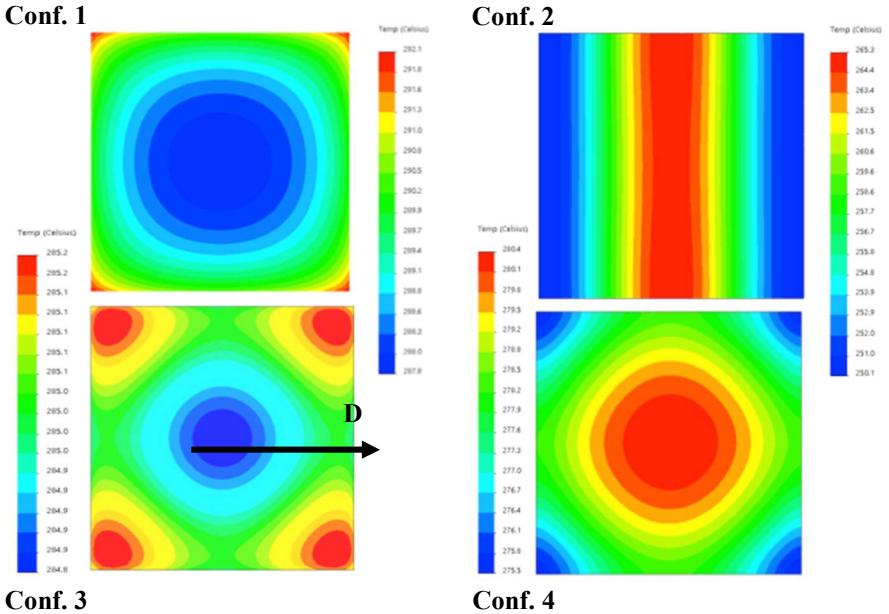

Fig. 6. Temperature distribution on the face of the HFC connected to the TE module

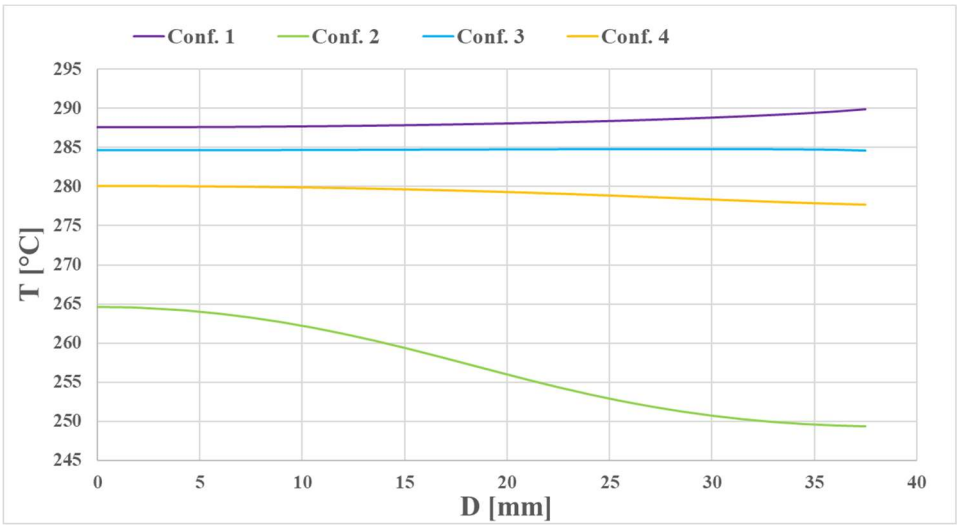

Fig. 7. HFC surface to cell temperature distribution along axial direction

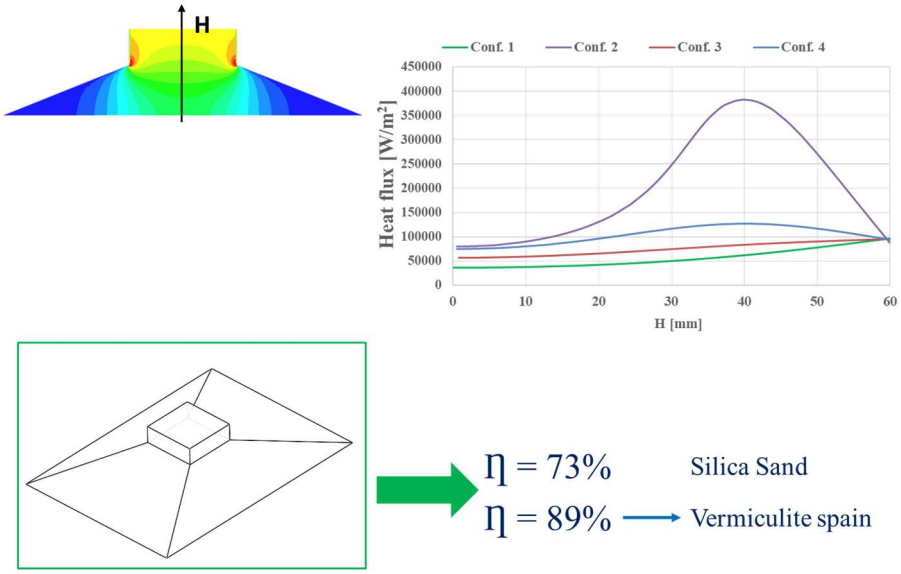

Fig. 8. Calculated Heat flux longitudinal profile for the HFC.

On the cold side of the HFC, the heat flux must be removed by the water coolant flow. A small circulation pump is taking cold water from the lower (colder) part of the storage tank and circulating it with a velocity of about 3 m/s across the water cooler. This last has an optimized design allowing to reach h = 5000 W/(m2°C); this allows to remove the large heat flux of about 90 kW/m2 with a temperature

difference of about 18°C. The cooling flow rate per TE module is mcw = 0.067 kg/s = 24 kg/h. For the whole fireplace assembly with 7 modules, the pump flow rate would be about 170 kg/h (this is less than half the hot water reservoir capacity).

5. CONCLUSIONS

An innovative design thermo-electric fireplace was designed, using radiative heat transfer to ensure high heat flux conditions on the thermoelectric modules. A heat flux concentrator HFC was used to intensify the heat flux on the TE modules, and water cooling (using the water storage capacity and supporting heat production for household heating) allows to maintain the required effective heat removal on the TE cold side. A radiation model including detailed view factors for the radiation chamber, and iterative adjustment of the glass window transmissivity (depending on wavelength and on the calculated equivalent flame temperature) was applied, and 3-D finite element calculations of the HFC allowed to obtain a high efficiency for this device and an overall compact and packaged design.
The solution is conceived as a simple plug-in substitution of the current refractory-lined fireplace design; for a typical fireplace with a heat rating of 26 kWt, it should allow to produce about 140 W of thermo-electric power. This can be a significant contribution for off-grid households equipped with photovoltaic electricity production, which depend fully on batteries or diesel generators after daylight. The whole system is thought as a customer catalogue add-on to the current OffGridBox ® offer, with an expected cost increase with respect to the heat-only fireplace of about 1000 €.

ACKNOWLEDGMENTS

This work was developed under the frame of a long-term cooperation among La Fabbrica del Sole SCRL, University of Florence and OffGridBox®.

NOMENCLATURE

A	Surface, m2
cp	Constant-pressure specific heat, J/(kg K)
D	Diameter, m
E	Radiation flux, W/m2
h	Heat transfer coefficient, W/(m2 K)
k	Conductivity, W(m K)
$\dot{m}$	Mass flow rate, kg/s
Q	Heat rate, W

S	Surface, m2
T	Temperature, K

Greek symbols

α	Absorption coeffecient
ε	Emissivity
λ	Wavelength, m
η	Efficiency
ρ	Reflectivity
σ	Stefan-Boltzmann constant
τ	Transmissivity

Subscripts and superscripts

a	Air (ambient)
C	Cold side (TE module)
c	Contact
ci	Cast Iron
Cu	Copper
cw	Cooling water
f	Flame
g	Gas (combustion products)
gw	Glass window
H	Hot side (TE module)
p	Wall
ov	Overall
ref	Refractory
TE	Thermo-Electric (module)
VP	Vertical plate (natural convection)
w	Wood
0	Flame (radiating cylinder)
1…6	WALL INDEX

REFERENCES

1. Lund, H, Ostergaard, PA, Connolly, P and Van Mathiesen, B 2017. Smart Energy and Smart Energy Systems. Energy.
2. Ackermann, T, Andersson, G and Soder, L 2001. Distributed generation: a definition. Electric Power Systems Research, 57, 195-204.
3. SolarPower Europe Global Market Outlook for Solar Power, 2018-20; available at: http://www.solarpowereurope.org/global-market-outlook-2018-2022/ (accessed Febr. 24th, 2019).
4. Terna, Bilancio Nazionale Energia Elettrica, 2017; available at: http://www.terna.it/it-it/sistemaelettrico/statisticheeprevisioni/bilancienergiaelettrica/bilancinazionali.aspx (accessed Febr. 24th, 2019).
5. https://www.offgridbox.com/company (visited February 24th, 2019).
6. He, W, Zhang, G, Zhang, X, Ji, J, Li, G and Zhao, X 2015. Recent development and application of thermoelectric generator and cooler. Applied Energy, 143, 1-25.
7. Champier, D, Bedecarrats, JP, Rivaletto, M and Strub, F 2010. Thermoelectric power generation from biomass cook stoves. Energy 35, 935–942.
8. Champier, D, Bedecarrats, JP, Kousksou, T, Rivaletto, M, Strub, F and Pignolet, F 2011. Study of a TE (thermoelectric) generator incorporated in a multifunction wood stove. Energy 36, 1518-1526.
9. Zheng, XF. Yan, YY and Simpson, K 2013. Potential candidate for the sustainable and reliable domestic energy generation - Thermoelectric cogeneration system. Applied Thermal Engineering 53, 305-311.
10. Zheng, XF, Liu, CX, Boukhanouf, R, Yan, YY and Li, WZ 2014. Experimental study of a domestic thermoelectric cogeneration system. Applied Thermal Engineering 62, 69-79.
11. Barma, MC, Riaz, M, Saidur, R and Long, BD 2015. Estimation of thermoelectric power generation by recovering waste heat from Biomass fired thermal oil heater. Energy Conversion and Management 98, 303–313.
12. Montecucco, A and Knox, AR 2014. Accurate simulation of thermoelectric power generating systems. Applied Energy 118, 166–172.
13. Montecucco, A, Siviter, J and Knox, AR 2015. Constant heat characterisation and geometrical optimisation of thermoelectric generators. Applied Energy 149, 248–258.
14. Bianchini, A, Pellegrini, M and Saccani, C 2014. Thermoelectric cells cogeneration from biomass power plant. Energy Procedia 45, 268 – 277.
15. Nuwayhid, RY, Rowe, DM and Min, G 2003. Low cost stove-top thermoelectric generator for regions with unreliable electricity supply. Renewable Energy 28 (2003) 205–222.

16. Nuwayhid, RY, Shihadeh, A and Ghaddar, N 2005. Development and testing of a domestic woodstove thermoelectric generator with natural convection cooling. Energy Conversion and Management 46, 1631–1643.
17. Lertsatitthanakorn, C 2007. Electrical performance analysis and economic evaluation of combined biomass cook stove thermoelectric (BITE) generator. Bioresource Technology 98, 1670–1674.
18. Rinalde, GF, Juanico, LE, Taglialavore, E, Gortari, S and Molina, MG 2010. Development of thermoelectric generators for electrification of isolated rural homes. International Journal of Hydrogen Energy, 3, 5, 5818-5822.
19. Faraji, AY, Goldsmid, HJ, Dixon, C and Akbarzadeh, A 2015. Exploring the prospects of thermoelectric power generation in conjunction with a water heating system. Energy, 90(2):1569–74.
20. Du, Q, Diao, H, Niu, Z, Zhang, G, Shu, G and Jiao, K 2015. Effect of cooling design on the characteristics and performance of thermoelectric generator used for internal combustion engine. Energy Convers Manage 101:9–18.
21. Liu, Ch, Chen, P and Li, K 2014. A 500W low-temperature thermoelectric generator: design and experimental study. Int J Hydrogen Energy, 39(28):15497–505.
22. Sornek, K, Filipowicz, M and Rzepka, K 2016. The development of a thermoelectric power generator dedicated to stove-fireplaces with heat accumulation systems. Energy Conversion and Management, 125, 185-193.
23. Ding, LC, Meyerheinrich, N, Tan, L, Rahaoui, K, Jain, R and Akbarzadeh, A 2017. Thermoelectric power generation from waste heat of natural gas water heater. Energy Procedia, 110.
24. Obernberger, I, Weiss, G and Kossl, M 2018. Development of a new micro CHP pellet stove technology. Biomass and Bioenergy, 116, 198-204.
25. Bueters, KA, Cogoli, JG and Habelt, WW 1975. Performance prediction of tangentially fired utility furnaces by computer model. International Symposium on Combustion, Volume 15, Issue 1, Pages 1245-1260.
26. https://www.crystran.co.uk/optical-materials/silica-glass-sio2
27. Wedding, B 1975. Measurements of High-Temperature Absorption Coefficients for Glass. Journal of the American Ceramic Society, 58 (3/4), 102-105.
28. http://hi-z.com/product/hz-20-thermoelectric-module-80-power/ (accessed November 30th, 2019).

Editor received the manuscript:04.12.2019